Bearing Capacity of Two-Layered Clay Based On Strain-Stabilised Fem and Conic Programming

Thien M.VO
University of Technology, Ho Chi Minh City, Vietnam
thienk94@gmail.com

Hoang C. NGUYEN
University of Technology, Ho Chi Minh City, Vietnam
nchoangoxf@gmail.com

Linh A. LE
University of Technology, Ho Chi Minh City, Vietnam
linhbkxd@gmail.com

An N. CHAU
University of Technology, Ho Chi Minh City, Vietnam
cnan@hcmut.edu.vn

ABSTRACT

Upper-bound limit analysis will be applied to determine the bearing capacity of footing resting on two-layered clays. The soil is modelled by a perfectly-plastic Mohr-Coulomb model. Cell-based smoothed finite element method (CS-FEM) is used to approximate the kinematically admissible velocity fields. The discretised optimisation problem is formulated as a problem of minimising a sum of Euclidean norms so that it can be solved using an efficient second order cone programming algorithm.

Keywords: *upper-bound limit analysis, Bearing capacity, CS-FEM, SOCP.*

INTRODUCTION

The well-known mechanism of Prandt (1920) was used popularly to determine bearing capacity of footing strip on homogenous soil. This failure mechanism, however, can not be applied for two-layer soil such as two-layer clays or sand on clay. In this paper, upper-bound limit analysis was applied to determine collapse load and shape of soil when it collapsed through solving optimisation problem established from upper-bound formulation. By applying it, the ultimate load and displacement fields corresponding to two-layer clays collapse will be determined.

This problem was researched by many authors in the past such as: Brown & Meyerhof (1969), Meyerhof & Hanna (1978) and especially R. S. Merifield & S. W.Sloan and H. S.Yu (1998), who applied upper-bound theorem using standard finite element method and linear programming to evaluate the collapse load. However, the main drawback of applying linear programming is the variations as well as the number of constraints increasing dramatically causing disadvantages solving optimisation problem. In this paper, a new numerical procedure using upper-bound limit analysis will be employed to estimate the bearing capacity of soil. The kinematically admissible velocity fields corresponding to the soil under footing collapsed were determined by solving optimisation problems which were formulated as a standard second-order cone programming via commercial or in-house optimisation packages . The results obtained will be compared with other authors in both cases depending on the properties of two clays.

DEFINITION OF THE PROBLEM

The footing strip with the width B resting on two-layer clays is illustrated in Figure 1. The properties of soil are the undrained shear strength c_{u1} and the height H of the first clay over the second one with undrained shear strength c_{u2} and infinity depth.

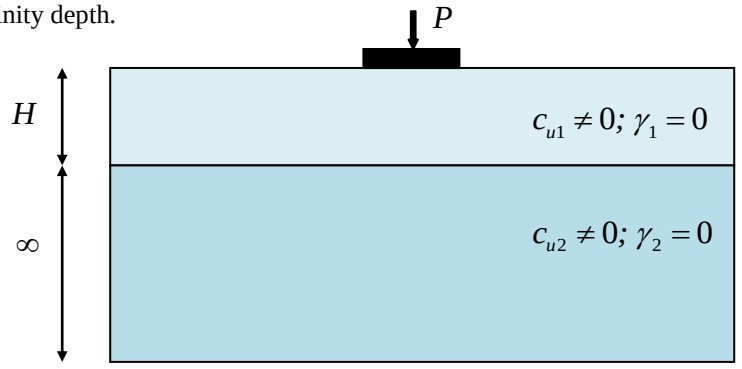

Figure 1: The footing strip resting on two-layer clays

With homogenous soil, the bearing capacity was formulated by the well-known following operation

$$q_{ult} = cN_c \qquad (1)$$

However, for this case, two-layer clays, the formulation is written as:

$$q_{ult} = c_{u1}N_c^* \qquad (2)$$

Where N_c^* denoting for bearing capacity factor depends on both ratio $\frac{H}{B}$ and $\frac{c_{u1}}{c_{u2}}$

UPPER-BOUND LIMIT ANALYSIS FORMULATION

Consider a rigid-perfectly plastic body of area $\Omega \in R^2$ with boundary Γ, which is subjected to body forces $\boldsymbol{f}$ and to surface tractions $\boldsymbol{g}$ on the free portion Γ_t of Γ. The constrained boundary Γ_u is fixed and $\Gamma_u \cup \Gamma_t = \Gamma$, $\Gamma_u \cap \Gamma_t = \varnothing$. Let $\dot{\boldsymbol{u}} = [\dot{u} \ \dot{v}]^T$ be plastic velocity or flow fields that belong to a space U of kinematically admissible velocity fields. Where $\dot{u}$ and $\dot{v}$ are the velocity components in the x and y directions respectively. The strain rates $\dot{\boldsymbol{\varepsilon}}$ can be expressed by relations

$$\dot{\boldsymbol{\varepsilon}} = \begin{bmatrix} \dot{\varepsilon}_{xx} \\ \dot{\varepsilon}_{yy} \\ \dot{\gamma}_{xy} \end{bmatrix} = \nabla \dot{\boldsymbol{u}} \tag{3}$$

with ∇ is the differential operator

$$\nabla = \begin{bmatrix} \dfrac{\partial}{\partial x} & 0 \\ 0 & \dfrac{\partial}{\partial y} \\ \dfrac{\partial}{\partial y} & \dfrac{\partial}{\partial x} \end{bmatrix} \tag{4}$$

The external work rate associated with a virtual plastic flow $\dot{\boldsymbol{u}}$ is expressed in the linear form as

$$W_{ext}(\dot{\boldsymbol{u}}) = \int_{\Omega} \boldsymbol{f}^T \dot{\boldsymbol{u}} d\Omega + \int_{\Gamma_t} \boldsymbol{g}^T \dot{\boldsymbol{u}} d\Gamma \tag{5}$$

The internal plastic dissipation of the two-dimensional domain Ω can be written as:

$$W_{int}(\dot{\boldsymbol{\varepsilon}}) = \int_{\Omega} D(\dot{\boldsymbol{\varepsilon}}) d\Omega \tag{6}$$

where the plastic dissipation $D(\dot{\boldsymbol{\varepsilon}})$ is defined by

$$D(\dot{\boldsymbol{\varepsilon}}) = \max_{\psi(\sigma) \le 0} \boldsymbol{\sigma}.\dot{\boldsymbol{\varepsilon}} = \boldsymbol{\sigma}_{\varepsilon}.\dot{\boldsymbol{\varepsilon}} \tag{7}$$

with $\boldsymbol{\sigma}$ represents the admissible stresses contained within the convex yield surface $\psi(\boldsymbol{\sigma})$ and $\boldsymbol{\sigma}_{\varepsilon}$ represents the stresses on the yield surface associated with any strain rates $\dot{\boldsymbol{\varepsilon}}$ through the plasticity condition.

The kinematic theorem of plasticity states that the structure will collapse if and only if there exists a kinematically admissible displacement field $\dot{\boldsymbol{u}} \in U$, such that:

$$W_{int}(\dot{\boldsymbol{\varepsilon}}) < \lambda^+ W_{ext}(\dot{\boldsymbol{u}}) + W_{ext}^0(\dot{\boldsymbol{u}}) \tag{8}$$

Where λ^+ is the collapse load multiplier, $W_{ext}^0(\dot{\boldsymbol{u}})$ is the work of any additional loads $\boldsymbol{f}_o$, $\boldsymbol{g}_o$ not subjected to the multiplier.

If defining $C = \{\mathbf{u} \in U | W_{ext}(\mathbf{u}) = 1\}$, the collapse load multiplier λ^+ can be determined by the following mathematical programming

$$\lambda^+ = \min_{\mathbf{u} \in C} \int_\Omega D(\boldsymbol{\varepsilon}) d\Omega - W_{ext}^0(\mathbf{u}) \tag{9}$$

CELL-BASED SMOOTHED FINITE ELEMENT METHOD (CS-FEM)

The essential idea of the cell-based smoothed finite element method (CS-FEM) combining the existing finite element method (FEM) with a strain smoothing scheme. In CS-FEM, the problem domain is discretised into elements as in FEM, such as $\Omega = \Omega^1 \cup \Omega^2 \cup ..... \cup \Omega^{nel}$ and $\Omega^i \cap \Omega^j = \varnothing, i \neq j$, and the displacement fields are approximated for each element as

$$u^h(x) = \sum_{I=1}^{n} N_I(x) d_I \tag{10}$$

where n is the number of nodes per element and $d_I = \left[u_I v_I\right]^T$ is the nodal displacement vector.

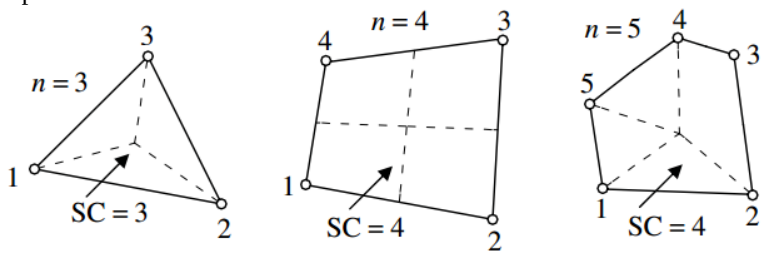

Figure 2: Smoothing cells for various element types: triangular element (left) is subdivided into three sub-triangular smoothing cells, quadrilateral element (middle) is partitioned into four subcells and polygonal element (right) subdivided into the shape of triangular and quadrilateral smoothing cells.

Elements are then subdivided into several smoothing cells, such as $\Omega^e = \Omega^e{}_1 \cup \Omega^e{}_2 \cup .... \cup \Omega^e{}_{nc}$ as shown in Figure 2, and smoothing operations are performed for each smoothing cell (SC). A strain smoothing formulation is given by [11]

$$\begin{aligned} \tilde{\boldsymbol{\varepsilon}}^h(x_C) &= \int_{\Omega^e c} \boldsymbol{\varepsilon}^h(x) \varphi(x, x - x_c) d\Omega \\ &= \int_{\Omega^e c} \nabla \mathbf{u}^h(x) \varphi(x, x - x_c) d\Omega \end{aligned} \tag{11}$$

where $\tilde{\varepsilon}^h$ is the smoothed value of strains ε^h for smoothing cell $\Omega^e{}_C$, and φ is a distribution function or a smoothing function that has to satisfy the following properties [11, 12]

$$\varphi \geq 0 \qquad and \qquad \int_{\Omega^e{}_C} \varphi d\Omega = 1 \tag{12}$$

For simplicity, the smoothing function φ is assumed to be a piecewise constant function and is given by

$$\varphi(x, x - x_C) = \begin{cases} 1/A_C, & x \in \Omega^e{}_C \\ 0 \quad , & x \notin \Omega^e{}_C \end{cases} \tag{13}$$

where A_C is the area of the smoothing cell $\Omega^e{}_C$

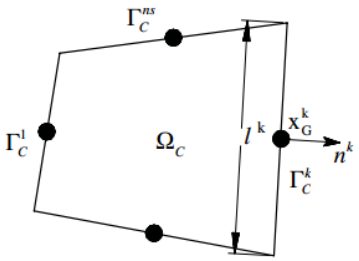

Figure 3: Geometry definition of a smoothing cell

Substituting equation (11) into equation (9), and applying the divergence theorem, one obtains the following equation

$$\begin{aligned} \tilde{\varepsilon}^h(x_C) &= \frac{1}{A_C} \int_{\Omega^e{}_C} \nabla \mathbf{u}^h(x) d\Omega \\ &= \int_{\Gamma_C} n(x) \mathbf{u}^h(x) d\Gamma \end{aligned} \tag{14}$$

where Γ_C is the boundary of $\Omega^e{}_C$ and n is a matrix with components of the outward surface normal given by

$$n = \begin{bmatrix} n_x & 0 \\ 0 & \mathrm{n_y} \\ \mathrm{n_y} & n_x \end{bmatrix} \tag{15}$$

Introducing a finite element approximation of the displacement fields, the smooth version of the strain rates can be expressed as

$$\dot{\tilde{\varepsilon}}(x_C) = \mathbf{B}\dot{\mathbf{d}} \tag{16}$$

where

$$\dot{\mathbf{d}}^T = [\dot{u}_1, \dot{v}_1, \ldots \dot{u}_n, \dot{v}_n]$$

$$\tilde{\mathbf{B}}=\begin{bmatrix} \tilde{N}_{1,x}(x_C) & 0 & \dots & \tilde{N}_{n,x}(x_C) & 0 \\ 0 & \tilde{N}_{1,y}(x_C) & \dots & 0 & \tilde{N}_{n,y}(x_C) \\ \tilde{N}_{1,y}(x_C) & \tilde{N}_{1,x}(x_C) & & \tilde{N}_{n,y}(x_C) & \tilde{N}_{n,x}(x_C) \end{bmatrix} \quad (17)$$

with

$$\begin{aligned} \tilde{N}_{I,\alpha}(x_C) &= \frac{1}{A_C}\int_{\Omega^e{}_C} N_I(x) n_\alpha(x)\, d\Gamma \\ &= \frac{1}{A_C}\sum_{k=1}^{ns} N_I(x_G{}^k) n_\alpha{}^k l^k, I = 1,2,\dots,n \end{aligned} \quad (18)$$

where $\tilde{N}_{I,\alpha}$ is the smoothed version of shape function derivative $N_{I,\alpha}$; n_s is the number of edges of a smoothing cell Ω_C as shown in Figure 2; $x_G{}^k$ is the Gauss point of boundary segment $\Gamma^k{}_C$ which has length l_x and outward surface normal n^k.

CS-FEM FORMULATION FOR PLANE STRAIN WITH MOHR–COULOMB YIELD CRITERION

In this study, the Mohr–Coulomb failure criterion is used

$$\psi(\sigma) = \sqrt{(\sigma_{xx}-\sigma_{yy})^2 + 4\tau_{xy}{}^2} + (\sigma_{xx}+\sigma_{yy})\sin\varphi - 2c\cos\varphi \quad (19)$$

where c is cohesion and φ is internal friction angle of soil.

The plastic strains are assumed to obey the normality rule

$$\dot{\varepsilon} = \dot{\lambda}\frac{\partial\psi}{\partial\sigma} \quad (20)$$

Where the plastic multiplier $\dot{\lambda}$ is non-negative.

Hence, the power of dissipation can be formulated as a function of strain rates for each domain i as

$$D(\dot{\varepsilon}) = cA_i t_i \cos\varphi \quad (21)$$

where

$$\|\boldsymbol{\rho}\|_i \le t_i \quad (22)$$

$$\boldsymbol{\rho} = \begin{bmatrix} \rho_1 \\ \rho_2 \end{bmatrix} = \begin{bmatrix} \dot{\varepsilon}_{xx} - \dot{\varepsilon}_{yy} \\ \dot{\gamma}_{xy} \end{bmatrix} \quad (23)$$

$$\dot{\varepsilon}_{xx} + \dot{\varepsilon}_{yy} = t_i \sin\varphi \quad (24)$$

Introducing an approximation of the displacement and using the smoothed strains, the upper-bound limit analysis problem for plane strain can be formulated as:

$$\lambda^+ = min \sum_{i=1}^{nSDxnel} cA_i t_i \cos\varphi \quad (25)$$

$$s.t\begin{cases} W_{ext}(\dot{\mathbf{u}}^h) = 1 \\ \dot{\mathbf{u}}^h = 0 \quad on\ \Gamma_u \\ \dot{\varepsilon}_{xx} + \dot{\varepsilon}_{yy} = t_i \sin\varphi \qquad i = 1,2,\text{K}\ , nel * nSD \\ \left\|\boldsymbol{\rho}\right\|_i \le t_i \qquad i = 1,2,\text{K}\ , nel * nSD \end{cases} \tag{26}$$

where nSD is the smoothing cell (all results in this paper were obtained by using nSD =1) and nel is the number of element in the whole investigated domain. And the fourth constraint in problem (26), resulting optimisation problem is cast in the form of a second-order cone programming (SOCP) problem so that a large-scale problem can be solved efficiently

NUMERICAL EXAMPLE

In this section, the performance of the new upper-bound formulation is assessed by applying it to predict the collapse load for a plane strain strip footing resting on two-layer clays. The bearing capacity factor N_c^* will be estimated for both cases: strong-over-soft clays and soft over-strong clays.

Due to symmetry, only half of the foundation is considered. The rectangular region of $L = 10B$ and $H = 8B$ was considered sufficiently large to ensure that rigid elements show up along the entire boundary. The punch is represented by a uniform vertical load and appropriate boundary conditions were applied as shown in Figure 1.

Footings on Strong Clay Overlying Soft Clay

The ratio of $\frac{H}{B}$ from 0.5 to 2 and ranging $\frac{c_{\text{u1}}}{c_{\text{u2}}}$ from 1.25 to 5 will be considered to investigate the influence of the depth of the strong clays on bearing capacity of footing. The results obtained will be shown in Table 1 by carrying out the computations using 4800 elements generated uniformly. According to the figures in Table 1, with the cases, the ratio has almost no effect on ultimate load putting on the footing foundation.

With all the cases $\frac{H}{B}$, the present results demonstrate that the bearing capacity declines when increasing the ratio $\frac{c_{\text{u1}}}{c_{\text{u2}}}$. This means that there is a reduction in bearing capacity if the top clay is harder than the rest ones . The present results are more accurate than the results obtained from analytical upper bound by Chen (1975), who assumed a simple circular failure mechanism. Moreover, the results obtained are better when comparing with the solution of Merifield , while the computations were carried out, in this paper, only using 4800 elements.

The velocity fields for the ratio $\frac{H}{B} = 0.5$ in both cases: $\frac{c_{u1}}{c_{u2}} = 2$ and $\frac{c_{u1}}{c_{u2}} = 5$ were shown in Figure 4. It is interesting to point out the domain of displacement fields become larger with increasing the ratio of $\frac{c_{u1}}{c_{u2}}$. This indicates that the soil strength profiles of top clays have a significant influence on the displacement fields, and it leads to a reduction in bearing capacity which was shown in Table 1. In term of strong-over-soft clay system, the failure mechanism will be changed with various of ratio $\frac{c_{u1}}{c_{u2}}$. This means that bearing capacity depends not only on the depth of the top clay but also on the relation of strong clay's strength with the other layer.

Table 1: Values of Bearing Capacity Factor N_c^* for the Case ($c_{u1} > c_{u2}$)

$\frac{H}{B}$	$\frac{c_{u1}}{c_{u2}}$	Values of bearing capacity factor N_c^*			
		Present method	**Upper bound Merifield (1999)**	**Upper bound Chen (1975)**	**Meyerhof and Hanna (1978)**
0.5	5	2.1659	2.44	2.55	1.82
	4	2.4678	2.74	2.83	2.11
	3.5	2.6679	2.93	3.02	2.32
	3	2.9105	3.16	3.25	2.59
	2.5	3.2254	3.47	3.54	2.97
	2	3.6614	3.89	3.94	3.51
	1.75	3.9444	4.16	4.20	3.90
	1.5	4.7204	4.48	4.52	4.41
	1.25	4.7204	4.94	4.93	5.10
0.75	5	2.7868	2.98	3.28	2.22
	4.5	2.9149	3.28	3.53	2.53
	4	3.0689	3.48	3.69	2.75
	3	3.4948	3.72	3.88	3.03
	2.5	3.7946	4.01	4.12	3.42

	2	4.1660	4.37	4.43	3.99
	1.75	4.4034	4.66	4.63	4.38
	1.5	4.6761	4.94	4.87	4.90
	1.25	4.9804	5.20	5.17	5.14
	5	3.4383	3.54	3.87	2.62
	4.5	3.5494	3.83	4.14	2.94
	4	3.6817	4.02	4.31	3.17
	3	4.0505	4.24	4.52	3.47
1	2.5	4.3190	4.50	4.77	3.87
	2	4.6471	4.82	5.11	4.46
	1.75	4.8308	5.00	5.32	4.86
	1.5	5.0336	5.18	5.53	5.14
	1.25	5.2271	5.30	5.53	5.14
	·	4.4900	4.56	5.18	3.41
	4.5	4.6666	4.84	5.46	3.77
	4	4.7576	4.98	5.53	4.02
	3	5.0021	5.15	5.53	4.35
1.5	2.5	5.1711	5.32	5.53	4.78
	2	5.2742	5.31	5.53	5.14
	1.75	5.2742	5.31	5.53	5.14
	1.5	5.2742	5.31	5.53	5.14
	1.25	5.2742	5.27	5.53	5.14
	5	5.2742	5.32	5.53	4.20
	4.5	5.2742	5.32	5.53	4.60
	4	5.2742	5.32	5.53	4.87
	3	5.2303	5.27	5.53	5.14
2	2.5	5.2303	5.27	5.53	5.14
	2	5.2303	5.27	5.53	5.14
	1.75	5.2303	5.26	5.53	5.14
	1.5	5.2303	5.26	5.53	5.14
	1.25	5.2303	5.26	5.53	5.14

The results obtained by the present method and other authors are shown in Figure 5 for comparison purposes.

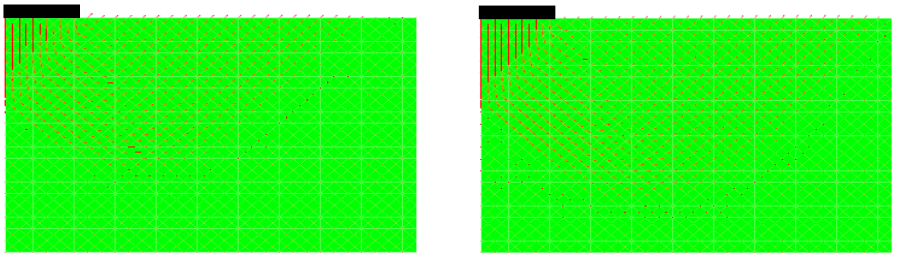

$a)\ \frac{c_{u1}}{c_{u2}} = 2$ $b)\ \frac{c_{u1}}{c_{u2}} = 5$

Figure 4: Displacement fields for strong over soft layers ($\frac{\mathbf{H}}{\mathbf{B}}$ = 0.5)

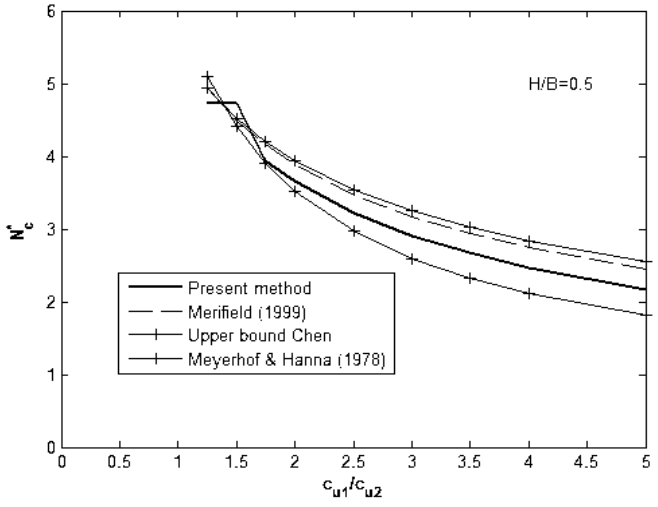

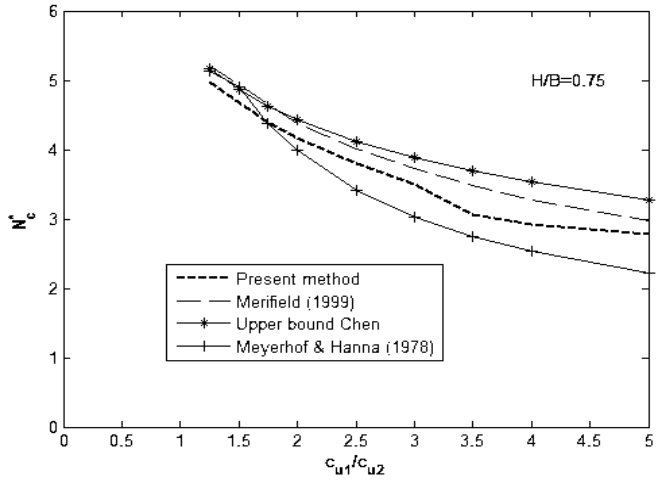
H/B=0.75
Present method
Merifield (1999)
Upper bound Chen
Meyerhof & Hanna (1978)
N_c^*
c_{u1}/c_{u2}

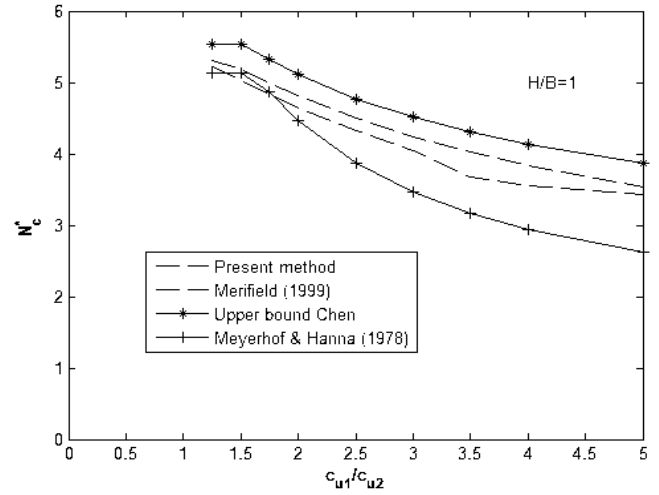
H/B=1
Present method
Merifield (1999)
Upper bound Chen
Meyerhof & Hanna (1978)
N_c^*
c_{u1}/c_{u2}

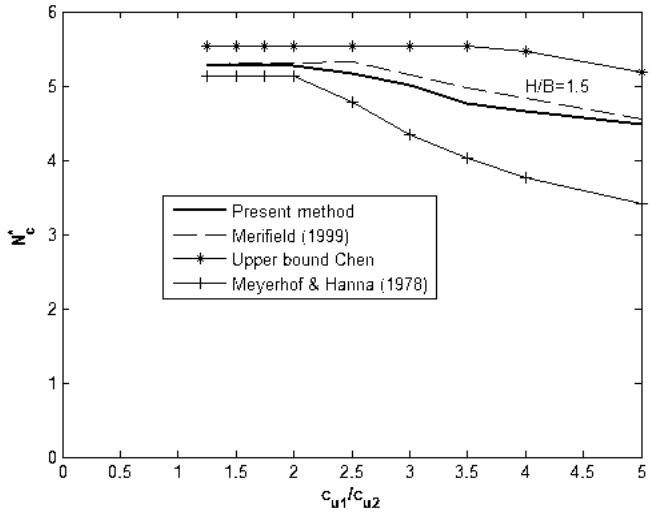

Figure 5: Variation of bearing capacity factor N_c^* (*H/B* = 0.5; *H/B* = 0.75 ; *H/B* = 1; *H/B* = 1.5)

Footings on Soft Clay Overlying Strong Clay

To estimate $\mathbf{N}_\mathbf{c}^*$, we set up $c_{u1} = 1$ in upper-bound limit analysis and ratios of c_{u2} ranging from 0.2 to 1 were considered to investigate the soil strength profiles effect on ultimate load which is also the value of $\mathbf{N}_\mathbf{c}^*$, in this case. The computations were carried out using 12800 elements and the results obtained were recorded in Table 2. According to Table 2, it is noted that the bearing capacity is independent of the ratio $\frac{c_{u1}}{c_{u2}}$.

To investigate the influence of the depth of soft clay as well as its strength relative to the underlying stronger clay on bearing capacity, the ratios $\frac{H}{B} = 0.25$ and $\frac{H}{B} = 0.5$ were considered with $\frac{c_{u1}}{c_{u2}} = 0.2$. The displacement fields and failure mechanisms for this case were shown in Figure 6 and Figure 7. It is clear to realise that the failure mechanism is likely to occur entirely in the soft clay.

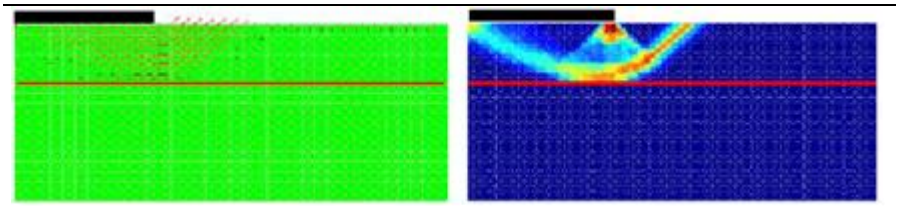

Figure 6: Displacement field and failure mechanism for the case $\frac{H}{B} = 0.25$ and $\frac{c_{u1}}{c_{u2}} = 0.2$

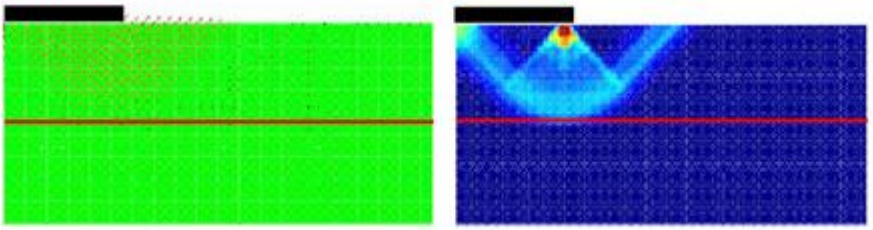

Figure 7: Displacement field and failure mechanism for the case $\frac{H}{B} = 0.5$ and $\frac{c_{u1}}{c_{u2}} = 0.2$

Table 2: Values of bearing capacity factor N_c^* for the case ($c_{u1} < c_{u2}$)

$\frac{H}{B}$	$\frac{c_{u1}}{c_{u2}}$	Values of bearing capacity factor N_c^*			
		Present method	Upper bound Merifield (1999)	Upper bound Chen (1975)	Meyerhof and Hanna (1978)
0.25	1	5.2081	5.32	5.53	5.14
	0.8	5.4797	6.25	6.57	5.52
	0.5	5.4797	6.52	7.61	6.00
	0.4	5.4797	6.52	7.61	-
	0.25	5.4797	6.52	7.61	-
	0.2	5.4797	6.52	7.61	-
0.5	1	5.2081	5.32	5.53	5.14
	0.8	5.2135	5.49	5.78	5.14

	0.5	5.2135	5.49	5.78	5.43
	0.4	5.2135	5.49	5.78	-
	0.25	5.2135	5.49	5.78	-
	0.2	5.2135	5.49	5.78	-
0.75	1	5.2081	5.32	5.53	5.14
	0.8	5.2135	5.36	5.53	5.14
	0.5	5.2135	5.36	5.53	5.14
	0.4	5.2135	5.36	5.53	-
	0.25	5.2135	5.36	5.53	-
	0.2	5.2135	5.36	5.53	-
1	1	5.2081	5.32	5.53	5.14
	0.8	5.2081	5.30	5.53	5.14
	0.5	5.2081	5.30	5.53	5.14
	0.4	5.2081	5.30	5.53	-
	0.25	5.2081	5.30	5.53	-
	0.2	5.2081	5.30	5.53	-

CONCLUSIONS

A procedure for upper-bound limit analysis based on cell-based smoothed finite element method and second order cone programming has been extended to computation of two layers soil foundation. By means of computational limit analysis, collapse multiplier and mechanism can be established efficiently. It has been shown that, when applying the CS-FEM to limit analysis problems, the size of optimisation problem is reduced. Various numerical examples were presented to show that the presented method can provide accurate and stable solutions with minimal computational effort.

ACKNOWLEDGEMENT

We would like to thank Dr Le Van Canh for his discussion as well as sharing code upper-bound limit analysis and plasticity.

REFERENCES

Brown J. D. and Meyerhof G. G. Experimental study of bearing capacity in layered clays. *International conference of soil mechanic and foundation engineering*, Mexico 2, 45-51.

Chen J. S , Wu C. T, and Belytschko T. (2000). Regularization of material instabilities by meshfree approximations with intrinsic length scales. *International Journal for Numerical Methods in Engineering*, *47*,1303-1322.

Le C. V, Gilbert M., and Askes H. (2009). Limit analysis of plates using the EFG method and second-order cone programming. *International Journal for Numerical Methods in Engineering*, *78*,1532-1552.Liu G. R, Nguyen Thoi T, and Lam K.Y. (2009). An edge-based smoothed finite element method (ES-FEM) for static, free and forced vibration analyses of solids. *Journal of Sound and Vibration*, 320:11001130.

Liu G. R. and Nguyen Thoi Trung. (2010). *Smoothed finite element methods*. CRC Press.

Makrodimopoulos A. and Martin C. M. (2006). Upper bound limit analysis using simplex strain elements and second-order cone programming. *International Journal for Numerical and Analytical Methods in Geomechanics*, *31*, 835- 865.

Merifield R.S.,Sloan S.W and Yu H.S. (1999). Rigorous plasticity solutions for the bearing capacity of two-layered clays. *Geotechnique,49 (4)*, 471-490. doi:10.1680/geot.1999.49.4.471

Mosek. (2011). The MOSEK optimization toolbox for MATLAB manual. *http://www.mosek.com*. *Mosek ApS*, version 6.0 edition.

Meyerhof G. G. and Hanna A. M. (1978). Ultimate bearing capacity of foundations on layer under inclined load. *Canadian Geotechnical Journal, 1*5, 565-572.

Prandtl L. 1920. Über die härte plastischer körper, *Göttingen Nachr. Math. Phys. Kl.*,**12**.

Shiau J. R, Lyamin A. V, and Sloan S. W.. (2003). Bearing capacity of a sand layer on clay by finite element limit analysis. *Geotechnique, 40*, 900-915.

W. F. Chen. (1975). *Limit analysis and soil plasticity*. Amsterdam: Elsevier .

Yoo J. W, Moran B, and Chen J. S . (2004). Stabilized conforming nodal integration in the natural-element method. *International Journal for Numerical Methods in Engineering*, *60*, 861-890.